ISSN 0036-0244, Russian Journal of Physical Chemistry A, 2024, Vol. 98, No. 14, pp. 3394–3403. © Pleiades Publishing, Ltd., 2024.

XXIV INTERNATIONAL CONFERENCE ON CHEMICAL THERMODYNAMICS IN RUSSIA (RCCT-2024)

Description of an *n*-Alkane/Water Phase Boundary in Presence of Polyethylene Glycol Ethers of Fatty Alcohols with the Aid of Coarse-Grained Multilayer Quasi-Chemical Model and Molecular Dynamics

P. O. Sorina[a] (ORCID: 0000-0003-3465-0469), M. A. Zolenko[a] (ORCID: 0009-0003-7488-4304), A. A. Vanin[a] (ORCID: 0000-0002-6722-4848), and A. I. Victorov[a,*] (ORCID: 0000-0001-9994-1297)

[a] *St. Petersburg State University, St. Petersburg, 199034 Russia*

**e-mail: victorov_a@yahoo.com*

Received August 20, 2024; revised August 20, 2024; accepted September 10, 2024

Abstract—Liquid interfaces are modeled for *n*-alkane + water systems with an without added non-ionic surfactants: polyethylene glycol ethers of fatty alcohols (C_nE_m). Coarse-grained molecular dynamic (MD) simulation with the MARTINI force field is combined with a coarse-grained version of a multilayer quasi-chemical model (MQM) of a non-uniform fluid mixture. The effect the choice of the monomer's unit size has on predicting the interfacial tension and mutual solubility of *n*-alkanes and water is demonstrated using the MQM. The interfacial tension's dependence on the length of the *n*-alkane chain and the structure of the added surfactant molecule are predicted satisfactorily. A predicted drop in the interfacial tension upon adsorption of the surfactant is consistent with the MD data. Liquid-liquid phase diagrams are calculated, and the non-uniform of the surfactant between the hydrocarbon and aqueous phases is described, depending on the ratio of the hydrophobic and hydrophilic parts of the C_nE_m molecule. The coarse-grained MQM is used to obtain normal and tangental pressure profiles and data on the local structure for flat and spherical phase boundaries. A conclusion is reached on the limited applicability of the coarse-grained approach within the MQM.

Keywords: coarse-grained approach, interfacial tension, water/oil, nonionic surfactants, quasi-chemical model, molecular dynamics, surface structure

DOI: 10.1134/S0036024424702959

INTRODUCTION

The properties of interphase boundaries play a key role in a number of different areas, including household and food chemistry, perfumery, oil production, drug delivery, isolating and purifying membrane proteins, and atmospheric phenomena.

Fluid phase boundaries are a wide class of interphase boundaries, for which a well-developed thermodynamic framework is available [1–4]. Molecular theories have been developed to describe the structure of non-uniform fluids that are applicable to molecules of similar sizes [4–6] and systems that contain chain molecules [7–14]. The main problem is that most of these theories do not describe local correlations between different chemical groups of complex organic molecules using only average values, and are therefore not applicable to systems that contain associating substances, particularly water and chain molecules that participate in hydrogen bonds. An exception is iSAFT, the version of the statistical theory of associated fluids (SAFT) [15] that was specially developed for inhomogeneous systems [11–14]). However, this theory requires solving a set of integral equations at each point of a non-uniform fluid, resulting in enormous computational costs. The theory also does not describe local orientations of functional groups, since it uses orientation-averaged distribution functions of a homogeneous fluid when constructing a correlation function for an inhomogeneous system [11, 13]. Molecular dynamic (MD) or Monte Carlo (MC) simulation remains today the major way of obtaining detailed structural information.

The above shortcomings of the theory can be overcome using the recently formulated multilayer quasi-chemical model (MQM) [16], which provides uniquely detailed information on the local structure of a non-uniform multicomponent fluid. This information includes: concentration profiles of chain molecule segments; orientation profiles of chemical bonds between each pair of segments; concentration profiles of different chemical groups; and orientations of pairs of contacting groups, particularly those of hydrogen

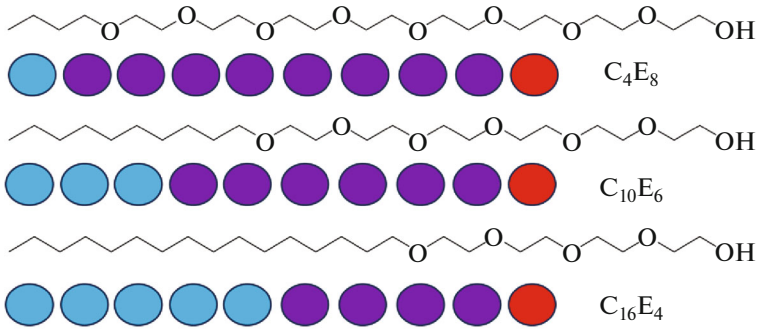

Fig. 1. Structural formulas and models of C_4E_8, $C_{10}E_6$, and $C_{16}E_4$ molecules in the MARTINI force field.

bonds. The model extends the approach first proposed by Smirnova [17, 18] (for the surface layer of a nonelectrolyte solution near a flat solid surface) to flat and curved fluid phase boundaries and mesoscale aggregates in a solution. It was shown [16] that the MQM can be used successfully to describe interphase boundaries in water + alkane model systems with added amphiphilic chain molecules, along with lamellar structures and reverse micelles in aqueous solutions of amphiphiles. However, the main limitation of the MQM is its requirement that all monomer units of chain molecules and solvent molecules be of the same size, substantially narrowing the range of systems that can be described.

A technique used successfully in MD modeling consists of switching to a coarse-grain description [19–21], when several force centers or molecules (e.g., H_2O in a MARTINI force field [22, 23]) are combined into one, thus reducing the required computer resources and expanding the and temporal scales of observation. Coarse-grained modeling is now in the arsenal of computer simulations that allow us to obtain structural details of very complex systems that remain inaccessible in other approaches.

The aim of this work was to test the similar procedure of coarse graining for the MQM model, in which several structural units are combined into one monomer particle to obtain monomers of roughly the same size for taking into account the steric interactions. Note that the model assumes allocation of contact areas on the surfaces of these monomers to allow for differences between the interaction of functional groups (particularly when describing hydrogen bonds).

Our chosen objects of study were flat interphase boundaries *n*-alkane/water with added polyethyleneglycol ethers of fatty alcohols $H(CH_2)_n(OCH_2CH_2)_mOH$ (C_nE_m). These nonionic surfactants are widely used as emulsifiers, detergents, and agents for separating membrane proteins. They are often considered archetypical nonionic surfactants [23, 24], since they are relatively easy to synthesize with different values of *n* and *m* that alter the hydrophilic–lipophilic balance. In solutions, C_nE_m form aggregated structures of varied morphology, and detailed experimental data have been acquired for them [25, 26]. C_nE_m aggregates [22, 23, 27] and water/oil interfaces in presence of these surfactants [24, 28] are widely studied by MD, employing both full-atom [22, 24, 28] and coarse-grained schemes [21, 22, 27], and reliable force fields have been developed for systems of this type [24, 25, 27].

In this work, coarse-grained MD simulation was done for a water/*n*-dodecane interface in presence of added surfactants with different hydrophobic/hydrophilic ratios (C_4E_8, $C_{10}E_6$, and $C_{16}E_4$). MQM modeling was done for mixtures containing water, *n*-alkanes of different carbon chain lengths, and an added C_nE_m surfactant. A brief description of the techniques is given in the next section, with a subsequent discussion of the results.

MODELING

Molecular Dynamics

The GROMACS 2019.2 package [29] with the MARTINI 3.0 coarse-grained force field [30, 31] was used in our MD simulation. Every four water molecules were replaced by one force center (WN), and each *n*-dodecane molecule was replaced by three force centers (C1) from the MARTINI 3.0 force field. In modeling surfactant molecules (Fig. 1), terminal groups CH_2–OH were represented by TP1 force centers (red); ethylene glycol fragments $-CH_2-O-CH_2-$, by SN1a force centers (purple); and fragments $-CH_2-CH_2-CH_2-$ and $H_3C-CH_2-CH_2-$ of hydrocarbon chains, by SC2 force centers (blue).

Each basic cell (Fig. 2) with two surfactant monolayers (64 surfactant molecules in each) separating the aqueous and dodecane phases contained 8192 water force centers (corresponding to 32768 water molecules) and 2730 dodecane molecules (8190 force centers). The linear dimensions of the cells along axes *X* and *Y* were identical, and periodic boundary condi-

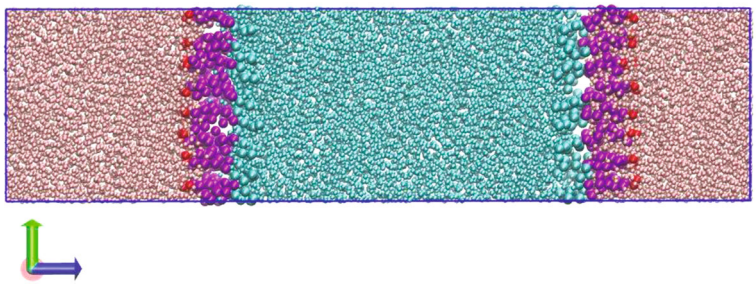

Fig. 2. Initial cell with $C_{10}E_6$ monolayers at the water/*n*-dodecane interfaces.

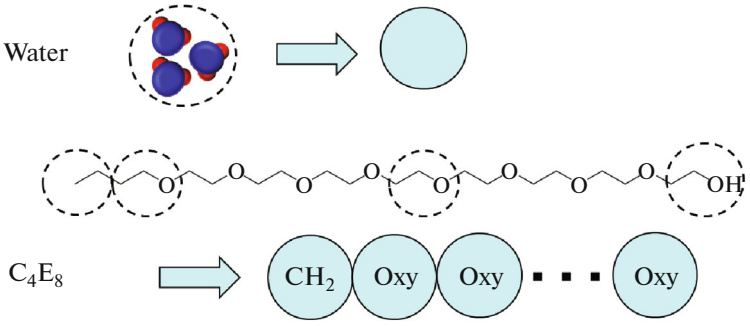

Fig. 3. Scheme for specification of the interacting monomer units in the coarse-grained MQM.

tions were imposed on each cell. The configurations were visualized using the VMD 1.9.3 program [32].

Simulation was done in three stages with a total duration of 100 ns for each MD run. A thermally and mechanically equilibrated system with specified values of temperature and surfactant adsorption at the interface was prepared in the first two stages. In the third and last stage, the calculated data were compiled and averaged.

In the first stage, mechanical equilibrium of a heterogeneous system with an atmosphere was obtained in the $NAP_{zz}T$ ensemble using a semi-isotropic barostat. The normal to interface component P_{zz} of the pressure tensor was set equal to 1 bar, and the compressibility was 3×10^{-4} bar^{-1}. The basic cell did not change its dimensions along axes *X* and *Y*, so the value of the area *A* of the interface remained constant. After the length of the cell along axis *Z* stopped changing, we moved on to the second stage: calculations using a special surface-tension barostat that determined the magnitude of both interfacial tension γ and the pressure normal to interfacial boundary P_{zz}. This allowed us to alter the value of surfactant adsorption at the interfacial boundary, since the dimensions of the cell changed along the directions of axes *X* and *Y*. Upon reaching a steady state, we moved on to the third stage (calculating in the canonical ensemble) with fixed values of temperature and the lengths of the sides of the basic cell. The interfacial tension was determined from the difference between the normal and tangental components of the pressure tensor [21, 24, 28].

Multilayer Quasi-Chemical Model

This model is an extension [16, 33] to flat and curved interfaces of fluid phases and micellar aggregates in solutions of the approach proposed by Smirnova [17, 18] for describing a non-uniform solution containing chain molecules near a flat interface with a solid. A non-uniform system is presented as layers of a given geometry containing structural units of chain molecules and monomeric molecules (quasilattice). Functional groups can be distinguished on the surfaces of the monomers, the orientational correlations between which are described within the Guggenheim quasi-chemical approximation. The infinite attraction between neighboring monomers of *r*-mers in this case ensures stoichiometric bonding of monomers in the chain, allowing us to describe inhomogeneities on scales much smaller than the length of an *r*-mer. Maximizing the general term of the partition function written for an inhomogeneous fluid mixture [16] allows us to obtain the equilibrium spatial distribution of monomeric structural units and their equilibrium orientations, revealing local concentrations and orientations of functional groups, chemical bonds of *r*-mers, and, particularly, the local orientations of hydrogen bonds in systems containing water. When describing compressible systems, vacant sites of the quasi-lattice are introduced as one type of monomer.

Table 1. Subdivision of *n*-alkanes and surfactant molecules into monomeric structural units

Monomer	*n*-Hexane	*n*-Decane	*n*-Dodecane	C_4E_2	C_6E_2	C_8E_3	C_6E_6	$C_{10}E_6$	C_4E_8
CH_2	3	5	6	1	2	3	2	4	1
Oxy	0	0	0	3	3	4	7	7	9

Vacancies are not introduced for incompressible systems that we consider in this work. The equations and the scheme of calculating the equilibrium structure of a non-uniform fluid were considered in detail in [16], and the expressions for determining thermodynamic properties, including interfacial tension and pressure profiles, were given in [33]. These expressions are very cumbersome and are not presented here. For a homogeneous isotropic fluid, the MQM reduces to the group quasi-chemical model [34, 35] that has been widely tested in calculating phase equilibria [36, 37].

As noted above, one of the most important limitations of the model is that the MQM assumes that all monomer units are the same size. This substantially narrows the range of systems, where the model is applicable. The aim of this work was to try to overcome this limitation by introducing a coarse-grained description.

Fragments of chain molecules and water molecules were combined into monomers using a coarse-grained description within the MQM, as it is shown in Fig. 3. The chains of *n*-alkanes and lipophilic tails of surfactant molecules were in this case modeled by monomers of the same type, CH_2. Another type of effective monomers (Oxy) was used to represent the hydrophilic parts of the surfactant. Table 1 shows the sets of these monomeric units that represent the considered *n*-alkanes and surfactant molecules.

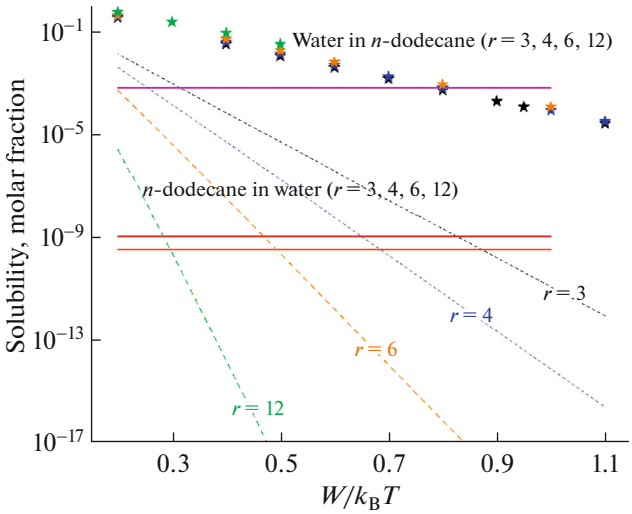

Fig. 4. Mutual solubility of water (asterisks) and *n*-dodecane (dashed line), calculated using the quasi-chemical bulk phase model as a function of the interchange energy W between the monomer units selected to model water and *n*-dodecane chains. All monomers have the same size. Different colors correspond to different numbers of monomer units in the dodecane chain: $r = 3, 4, 6, 12$. The experimental solubilities for $T = 298.15$ K [38] are shown as horizontal lines.

We cannot select monomer units that are exactly the same as in MD simulation, due to the notable difference in the sizes of the latter. There is a certain arbitrariness in specifying the monomeric units units, and we must adjust the values of the model parameters describing the interactions between these units in different sets. This is illustrated in Fig. 4, which presents results from calculating the mutual solubility of water and *n*-dodecane (represented as a trimer, tetramer, hexamer, or dodecamer), depending on the interchange energy of the selected monomer unit of dodecane and water. It can be seen that we can obtain a satisfactory description of both the water and hydrocarbon layers by choosing the trimer model for the *n*-dodecane molecule. When using a larger number of monomers, we must reduce the interchange energy to achieve adequate values of the solubility of *n*-dodecane in water.

Choosing a tetramer model for dodecane and calculating the mutual solubility for water and *n*-alkanes of different carbon chain lengths at $\frac{W}{k_BT} = 0.7$, we obtain the results shown in Fig. 5. In qualitative agreement with the experiment, the solubility of *n*-alkanes in water falls logarithmically as the length of chains increases. This solubility is orders of magnitude lower than the solubility of water in *n*-alkanes. In contrast, the latter depends weakly on the length of the alkane chains and grows along with it. We would therefore expect that a valid choice of a monomer unit is possible for the considered range of systems within the coarse-grained MQM.

It is interesting to consider how a particular choice of the MQM parameters affects the subsequent calculations of the interfacial tension. Table 2 contains the interfacial tensions for a water–dodecane system calculated for different choices of the monomer unit size. The interchange energies are in this case chosen to ensure solubility of *n*-dodecane in water that is close to the experimental value. Note that the value $\tilde{W} = 0.815$ from from table is close to the estimate obtained by combining the parameters of the MARTINI potential well depth ($\tilde{W} = 0.791$).

As discussed in [33], the value of the interfacial tension $\gamma = k_BT\tilde{\gamma}\frac{6}{\pi D^2}$ obtained from the model depends on the area per monomer, and thus on the

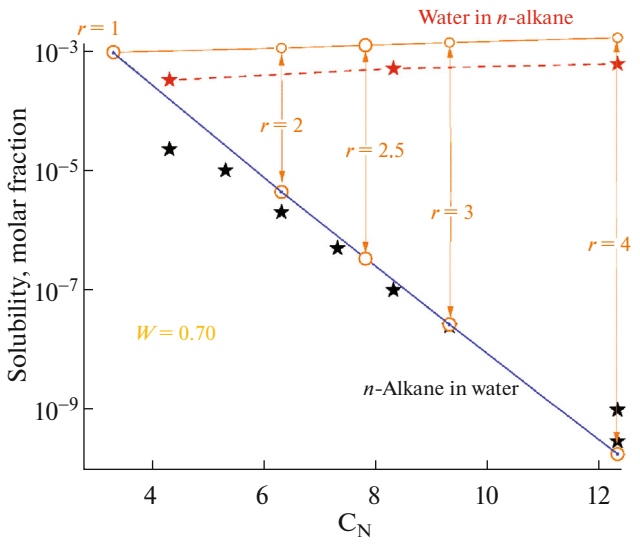

Fig. 5. Mutual solubility of water and *n*-alkanes (circles) of different carbon chain C_N lengths, calculated with the quasi-chemical model of the bulk phase. The fragment corresponding to three carbon atoms of the skeleton was chosen as the effective monomer. The interchange energy $\frac{W}{k_BT} = 0.7$. The asterisks show experimental values of mutual solubility at $T = 298.15$ K [38]. The blue line represents analytical calculations based on the limit values of the activity coefficients for the specified values of the model parameters. Note that for the monomer + *r*-mer system with one type of contact sites, the infinite dilution activity coefficient for the *r*-mer in the monomer in the quasi-chemical model is written analytically: $\gamma^{\infty}_{r\text{-mer}} = r\left[e^{\frac{W}{k_BT}}\sqrt{\frac{zq}{zr}}\right]^{zq}$, where $zq = r(z-2)+2$ is the number of contacts of the linear or branched *r*-mer with the nearest neighbors, and $z = 10$ is the coordination number of the lattice.

choice of diameter D of the monomer unit. The volumes of the monomers in Table 2 correspond to diameters chosen to obtain the experimental value of the surface tension. It is obvious that except for $r = 6$, these volumes are non-physically small. (Let us recall that the volume per a molecule in liquid water is approximately 27 Å.) We used the monomer size corresponding to the $r = 6$ model in all calculations described below.

Table 2. Dimensionless interfacial tensions $\tilde{\gamma} = \gamma a/(k_BT)$ in the *n*-dodecane (*r*-mer) + water (monomer) system, calculated using the MQM for different choices of the monomer unit size and water–*n*-dodecane monomer exchange energy $\tilde{W} = \frac{W}{k_BT}$; $T = 298.15$ K. Here, a is the area of contact between the monomer and the adjacent quasi-lattice layer. The experimental value of the interfacial tension is 52.55 mN/m [39]

n-Dodecane (*r*-mer)	$\tilde{W}$	$\tilde{\gamma}$	Volume of monomer, Å^3
3	0.70	0.708	34.44
4	0.815	0.798	49.22
6	0.50	0.899	49.25

When describing interactions in systems with surfactants, the Oxy monomer surface of the hydrophilic chain is considered to be energetically heterogeneous because it has a part (Oxy(C)) corresponding to two methylene groups and a part (Oxy(O)) corresponding to oxygen. The ratio of the surfaces of these subgroups accessible to surrounding molecules is 2:1 for all Oxy monomers. An exception is the terminal monomer of the chain, in which the external surface of oxygen not bound to the second methylene group is larger. The ratio of these areas is estimated as 8 : 9 [35].

The interfaces between water and *n*-dodecane in presence of added C_nE_m were modeled earlier in the works of the Dutch school [40, 41] using the Scheutjens–Fleer lattice model, where Flory parameters of 2.0 and −1.6, respectively, were used to describe energetically unfavorable and favorable interactions between monomers [40]. These values were recalculated into the interchange energies in our model (Table 3) and are used below to model the surface properties.

Modeling the interphase boundaries with the MQM was preceded by calculating phase equilibria in the considered system using a quasi-chemical model of a uniform bulk fluid. The MQM was used to calculate the equilibrium structure and properties of the interfaces between the equilibrium phases, as in [16, 33].

The situation is considerably more complicated for mixtures containing surfactants than for water + *n*-alkane systems. Calculations using the bulk phase model yield two or three coexisting liquid phases in a ternary system. The hydrophobic–lipophilic balance, the type of phase diagram, and the properties of the interphase boundaries depend on the ratio of the lengths of the hydrophilic and hydrophobic subchains of the C_nE_m molecule. According to the model's prediction, $C_{10}E_6$ does not exhibit phase split when mixed with *n*-dodecane at 298 K, but it is partially miscible with water. C_4E_8, on the contrary, is unlimited soluble in water and forms two liquid fases with *n*-dodecane. In contrast, $C_{10}E_6$, is soluble in water and produces two liquid phases with *n*-dodec-

Table 3. Interchange energies used in modeling the surface properties of water + *n*-alkane + C_nE_m mixtures using the coarse-grained MQM

Monomer	CH_2	Oxy(C)	Oxy(O)	Water
CH_2	—	0.0	0.30	0.30
Oxy(C)	—	—	0.30	0.30
Oxy(O)	—	—	—	−0.16
Water	—	—	—	—

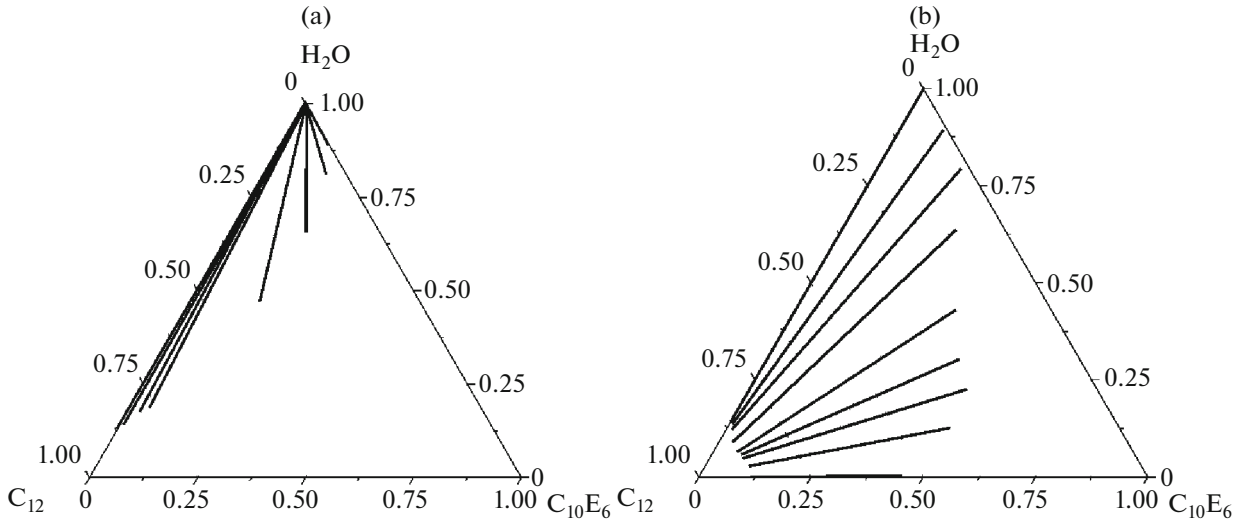

Fig. 6. Liquid–liquid equilibrium diagrams, calculated according to the quasi-chemical model in ternary systems (a) *n*-dodecane (C_{12}) + water + $C_{10}E_6$ and (b) *n*-dodecane (C_{12}) + water + C_4E_8. Straight lines show the nodes. The model parameters are from Table 3; $T = 298$ K.

ane. As expected, $C_{10}E_6$, which has a long hydrocarbon tail, partitions preferentially in the hydrocarbon phase (Fig. 6a). C_4E_8, which has an extended hydrophilic head, partitions preferentially in the water phase (Fig. 6b).

RESULTS AND DISCUSSION

MD Modeling

MD data on interfacial tensions as function of the adsorption of the surfactant are presented in Table 4. As expected, the interfacial tension falls as adsorption rises. The rate of the drop in the interfacial tension of the studied surfactants is similar, but they grows slightly along with the polyethylene glycol fragment of the molecule. The highest rate is for the *n*-butyl ether of octaethylene glycol.

The interfacial tension for the *n*-dodecane + water boundary with no surfactant ($\Gamma = 0$) is in good agreement with the available experimental data for a lower range of temperatures (50.00 ± 0.04 mN/m at 333 K and 53.54 ± 0.04 mN/m at 283 K) [39].

Table 5 presents data from MD simulation of the adsorption isotherms of $C_{10}E_6$ in the *n*-dodecane + water + $C_{10}E_6$ system at several temperatures. The interfacial tension fell monotonically as the temperature rose in the 0 to 1.5 nm^{-2} range of adsorption. The interfacial tension fell by an average of ~0.15 mN/m upon raising the temperature by 1 K. The temperature dependence of the interfacial tension for the *n*-dodec-

Table 4. Interfacial tensions in *n*-dodecane + water + C_nE_m systems, as function of the adsorption of surfactant at 353 K. The relative error in estimates of the interfacial tension in MD calculations is no more than 5%

$C_{10}E_6$		$C_{16}E_4$		C_4E_8	
Γ, nm^{-2}	γ, mN/m	Γ, nm^{-2}	γ, mN/m	Γ, nm^{-2}	γ, mN/m
0	53.8	0	53.8	0	53.8
0.36	50.4	0.39	50.2	0.38	49.4
0.85	39.7	0.93	40	0.77	40.7
1.00	35.3	1.00	37.7	1.00	33.2
1.16	31.5	1.24	29.6	1.13	30.2
1.43	18.8	1.49	20.1		
1.68	10.0	1.73	9.6		

Table 5. Interfacial tensions, as function of the adsorption of the surfactant at different temperatures in the *n*-dodecane + water + $C_{10}E_6$ system. The relative error in the interfacial tension estimates in MD calculations is no more than 5%

Temperature, K					
353		323		293	
Γ, nm^{-2}	γ, mN/m	Γ, nm^{-2}	γ, mN/m	Γ, nm^{-2}	γ, mN/m
0.0	53.8	0.0	57.4	0.0	61.3
0.36	50.4	0.43	53.3	0.61	54.3
0.85	39.7	0.98	39.3	1.10	39.9
1.00	35.3	1.00	39.6	1.66	20.0
1.16	31.5	1.28	28.4		
1.43	18.8	1.55	20.2		
1.68	10.0				

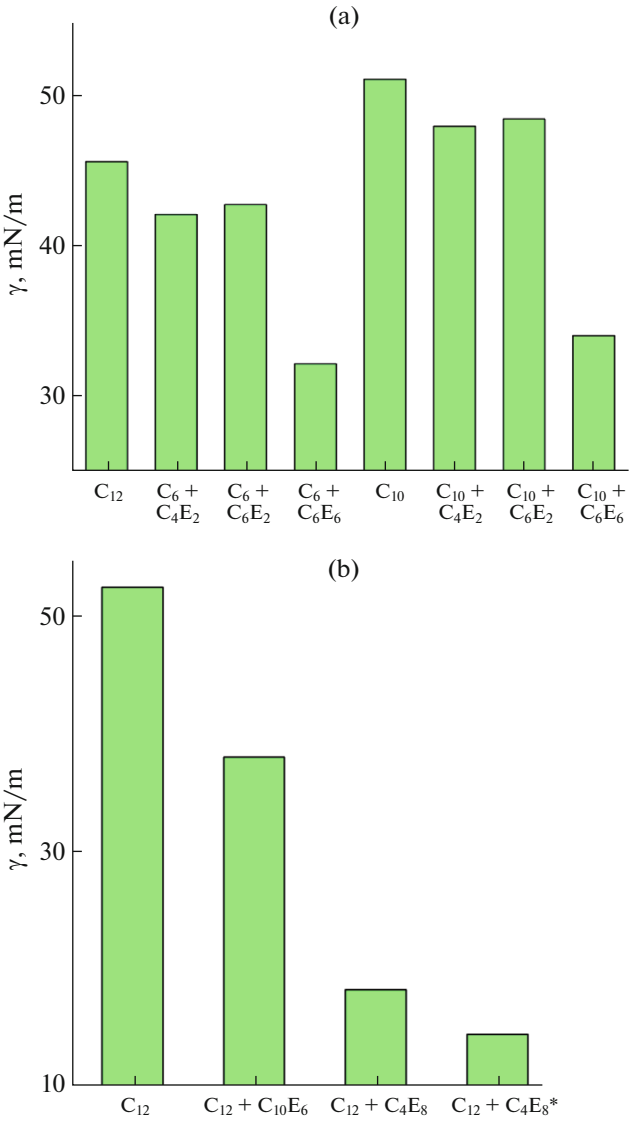

Fig. 7. Prediction of a drop in the interfacial tension of a flat water/*n*-alkane interface upon adding surfactant C_nE_m to (a) mixtures of water with *n*-hexane (C_6) and *n*-decane (C_{10}), and (b) a mixture of water with *n*-dodecane (C_{12}). The ratio of the mole fractions of the added surfactant and *n*-alkane in the hydrocarbon phase is 0.01 for all ternary systems, with the exception of the mixture marked with an asterisk, for which the ratio is 0.008. The model parameters are from Table 3. The lattice layer is 0.27 nm thick; $T = 298$ K.

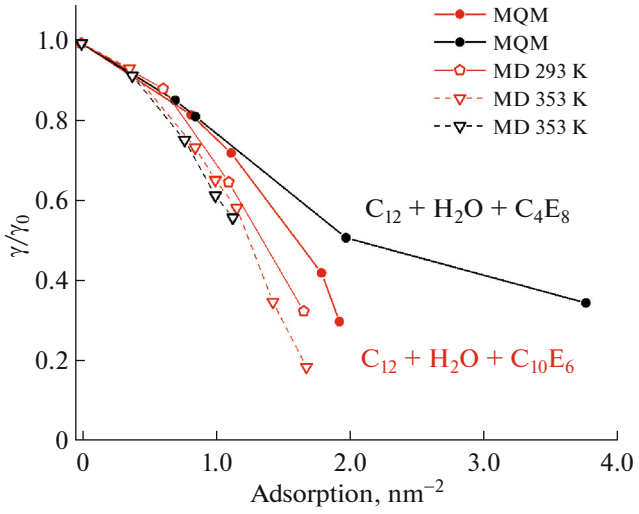

Fig. 8. Dependence of the relative decrease in the interfacial tension of the flat interface between the hydrocarbon and aqueous phases on the adsorption of the added surfactant in mixtures of water + *n*-dodecane (C_{12}) + $C_{10}E_6$ (red) and water + *n*-dodecane (C_{12}) + C_4E_8 (black). γ_0 is the interfacial tension in the system with no surfactant. Dots are MQM calculations for $T = 298$ K; other symbols are MD data.

ane + water system is much stronger than the one found experimentally [39]. In contrast to the grossly overestimated values of the interfacial tension that we obtained (the experimental value at 293 K was 52.83 mN/m [33]), MD simulation in the (N, A,P_N,T)-ensemble using the MARTINI force field and the DL_POLY 2.20 program underestimated the interfacial tension (43.6 ± 1.0 mN/m at 298 K) [21] by approximately the same amount, relative to the experimental data (52.55 ± 0.04 mN/m at 298 K [39]).

Modeling with the Coarse-Grained MQM

The interfacial tensions calculated for planar liquid–liquid interfaces in water + *n*-alkane and water + *n*-alkane + C_nE_m mixtures are shown in Fig. 7. The model correctly predicts a rise in interfacial tension as the length of the alkane chains grows and a drop upon adding a surfactant to the system. Lengthening the polar chains of surfactant molecules in this case enhances their effect (in agreement with the MD results), while a longer hydrocarbon tail somewhat reduces its efficacy. The experimental values of the interfacial tension for mixtures of water with *n*-hexane, *n*-decane, and *n*-dodecane with no added surfactant were 50.38, 51.98, and 52.55 mN/m, respectively [39]. We have to set an non-physically thin lattice layer (0.27 nm) to obtain the fairly close calculated values given in Figs. 7a, 7b.

The calculated dependence of the drop in the surface tension on the adsorption of surfactants at the interface is presented in Fig. 8. The predictions of the MQM are generally consistent with the results from MD. From this figure, it might seem that the surfactant with a shorter polyethylene glycol fragment of the molecule reduced the interfacial tension better. However, the adsorption of C_4E_8 was considerably higher with the same content of these surfactants in the bulk phase, and the interfacial tension was lower than in the system with $C_{10}E_6$.

Figure 9 illustrates the capabilities of the model in describing local characteristics of interfaces using the example of the water + *n*-hexane + C_6E_6 system. The

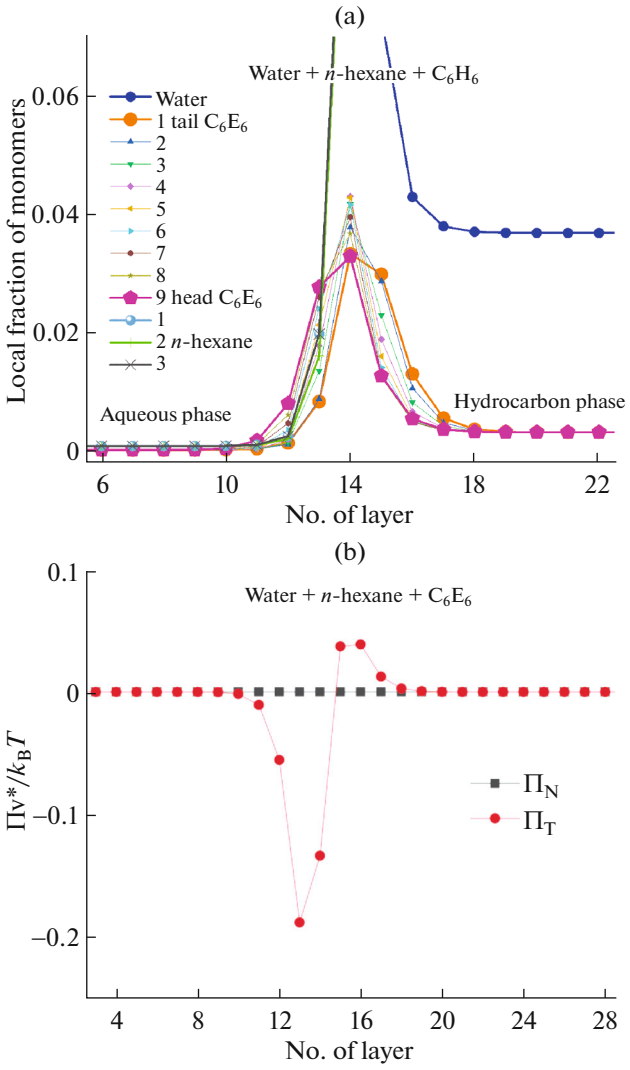

Fig. 9. Results from MQM predictions for a flat interface between the liquid phases in the mixture of water + *n*-hexane + C_6E_6. (a) Profiles of the local fraction of monomer segments of the molecules; the segments are numbered starting from the tail of the chains. (b) Profiles of the normal and tangential components of the osmotic pressure tensor excess with respect to the bulk phases. The model parameters are from Table 3; $T = 298$ K.

distribution profiles of monomer segments of molecules in the flat interfacial region (Fig. 9a) and the profiles of the normal and tangential components of the osmotic pressure (Fig. 9b) were predicted. The normal component did not change as it should have when passing through a flat boundary of mechanically equilibrium phases, and the tangential component indicates repulsion between surfactant tails near the hydrocarbon phase and tension in the part of the interfacial layer enriched in polar surfactant heads near the aqueous phase (Fig. 9a)

MQM allows us to trace the effect the molecular structure of the surfactant has on the pressure profile

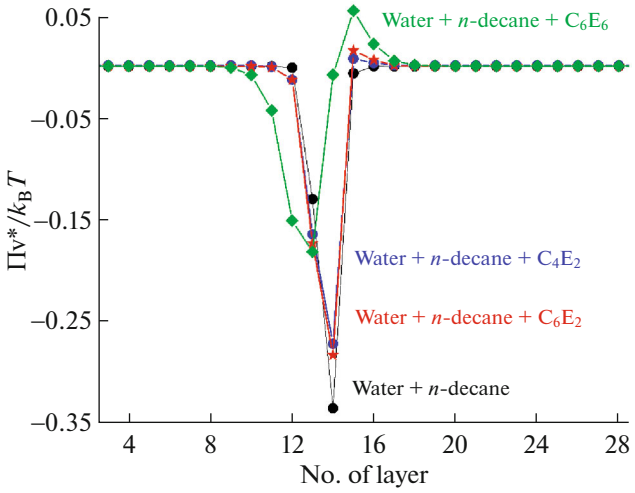

Fig. 10. Effect the surfactant structure has on the profile of the tangential component of the osmotic pressure for a flat liquid interface in water + *n*-decane + C_nE_m mixtures, predicted by the MQM. Model parameters are from Table 3, $T = 298$ K. ◆ water + *n*-decane + C_6E_6, ● water + *n*-decane + C_4E_2, ★ water + *n*-decane + C_6E_2, ● water + *n*-decane.

(Fig. 10), and thus on the interfacial tension. Figure 10 shows that elongation of the polar chain of the surfactant affects the tangential pressure profile much more than elongation of its tail, raising the repulsion of the tails (due to strong adsorption of the surfactant) from the side of the hydrocarbon phase and reducing the tension from the side of the aqueous phase.

Figure 11 presents results calculated for a spherical droplet of the aqueous phase surrounded by the hydrocarbon phase in the mixture with added surfactant according to the coarse-grained MQM. Figure 11a shows that the hydrocarbon phase, relative to the aqueous phase, was noticeably enriched in the surfactant, the non-polar tail of which was much longer than the polar part. Quite expectedly, the surfactant chains were adsorbed in the interphase region, turning their heads toward the aqueous droplet. The Laplace pressure difference inside and outside the spherical drop is clearly visible in Fig. 11b. The calculated radius of the droplet's surface of tension [42] lies approximately in the middle of the surface layer: $R_c = 11.76D$, where D is the thickness of one quasi-lattice layer. The dimensionless interfacial tension for the considered system ($\gamma a/(k_BT) = 0.448$) is close to but slightly lower than the interfacial tension ($\gamma a/(k_BT) = 0.450$) for a flat interface in this system with the same ratio of mole fractions of the added surfactant and *n*-alkane in the hydrocarbon phase (equal to 0.01).

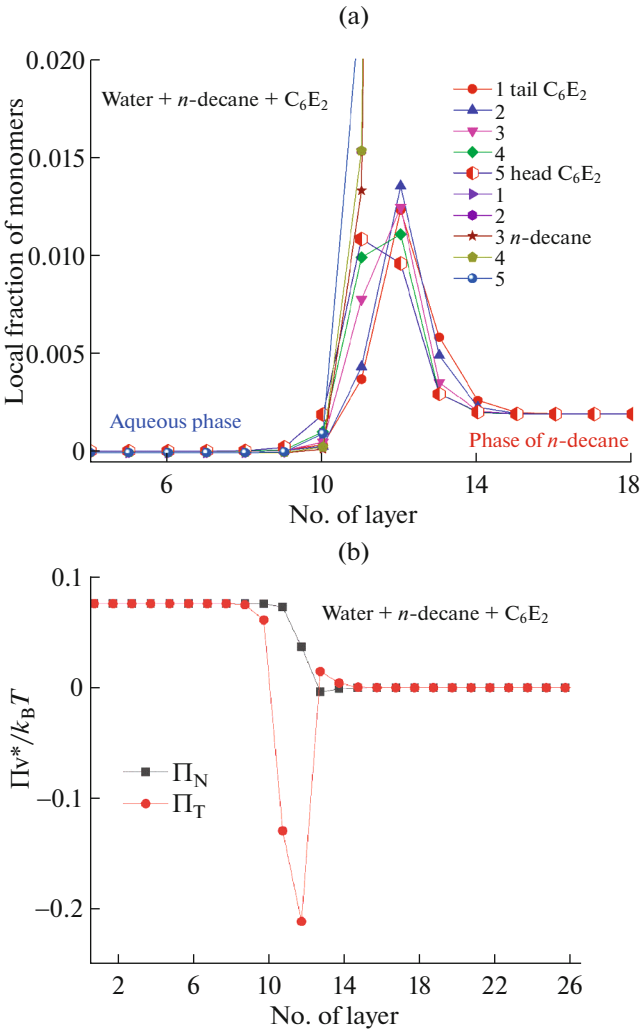

Fig. 11. Results from MQM predictions for a spherical water droplet in the hydrocarbon phase of water + *n*-decane + C_6E_2 system. (a) Profiles of the local fraction of monomer segments of molecules; the segments are numbered starting from the tail of the chains. The content of water in the hydrocarbon phase is around 3 mol %, so the water distribution profile is not visible in the graph of this scale. (b) Profiles of the normal and tangential components of the tensor of osmotic pressure, which is in excess relative to the bulk phase. The model parameters are from Table 3; $T = 298$ K.

CONCLUSIONS

Coarse-grained MD simulation with the MARTINI force field and a multilayer quasi-chemical model of a non-uniform fluid mixture (MQM) were used to describe interfaces between liquid phases for *n*-alkane + water systems with and without surfactant C_nE_m having different ratios of the lengths of hydrophobic and hydrophilic sub-chains. The coarse-grained description was tested within the MQM. The effect the choice of the monomer unit size had on predictions of the interfacial tension and mutual solubility of *n*-alkanes and water was demonstrated. Satisfactory results were obtained from predicting the dependence of the interfacial tension on the *n*-alkane chain length and on the structure of the added surfactant molecule. The predicted drop in interfacial tension upon adsorption of the surfactant was in good agreement with our MD data. The demonstrated possibility of adequately predicting the local structure and pressure profiles for interfacial boundaries, both flat and curved, should be considered an undoubted advantage of the developed version of the MQM. Note that the quasi-chemical model also allows us to predict phase diagrams that reflect the preferred partitioning of surfactants between the hydrocarbon and aqueous phases, depending on the ratio of the hydrophobic and hydrophilic parts of the C_nE_m molecule. However, we have to assume a non-physically thin lattice layer in order to obtain a quantitative description of interfacial tension, so the coarse-grained approach is applicable only partially within the MQM. It seems that a more promising way of further development of the MQM for expanding its applicability to a wider range of systems, is to develop a version of the model that allows for differences in the sizes of monomeric fragments of molecules.

ADDITIONAL INFORMATION

This paper is dedicated to the centennial of the Laboratory of Chemical Thermodynamics, Department of Chemistry, Moscow State University.

FUNDING

P.O. Sorina and A.I. Victorov thank the Russian Science Foundation, project 20-13-00038, for supporting research devoted to developing the MQM.

CONFLICT OF INTEREST

The authors of this work declare that they have no conflicts of interest.

REFERENCES

1. A. I. Rusanov, Russ. J. Gen. Chem. **92**, 539 (2022).
2. A. I. Rusanov, *Micelle Formation in Solutions of Surfactants* (Khimiya, St. Petersburg, 1992) [in Russian].
3. A. I. Rusanov, *Lectures on Thermodynamics of Surfaces* (Lan', St. Petersburg, 2013) [in Russian].
4. J. S. Rowlinson and B. Widom, *Molecular Theory of Capillarity* (Clarendon, Oxford, 1982).
5. J.-P. Hansen, and I. R. McDonald, *Theory of Simple Liquids with Applications to Soft Matter,* 4th ed. (Elsevier, Amsterdam, 2013).
6. S. M. Oversteegen, P. A. Barneveld, F. A. M. Leermakers, and J. Lyklema, Langmuir **15**, 8609 (1999).
7. A. Ben Shaul and W. Gelbart, in *Micelles, Membranes, Microemulsions and Monolayers,* Ed. by W. Gelbart,

A. Ben Shaul, and D. Roux (Springer, New York, 1994), p. 1.
8. J. M. H. M. Scheutjens and G. J. Fleer, J. Phys. Chem. A **83**, 1619 (1979).
9. G. J. Fleer, J. M. H. M. Scheutjens, and M. A. Cohen Stuart, Colloids Surf. **31**, 1 (1988).
10. J. G. J. L. Lebouille, R. Tuinier, L. F. W. Vleugels, et al., Soft Matter **9**, 7515 (2013).
11. S. Jain, A. Dominik, and W. G. Chapman, J. Chem. Phys. **127**, 244904 (2007).
12. C. P. Emborsky, K. R. Cox, and W. G. Chapman, J. Chem. Phys. **135**, 084708 (2011).
13. L. Wang, A. Haghmoradi, J. Liu, et al., J. Chem. Phys. **146**, 124705 (2017).
14. S. Xi, L. Wang, J. Liu, and W. G. Chapman, Langmuir **35**, 5081 (2019).
15. W. G. Chapman, J. Jackson, and K. E. Gubbins, Mol. Phys. **65**, 1057 (1988).
16. P. O. Sorina and A. I. Victorov, Langmuir **40**, 1577 (3) (2024). https://doi.org/10.1021/acs.langmuir.3c01741
17. N. A. Smirnova, Fluid Phase Equilib. **2**, 1 (1978).
18. N. A. Smirnova, Kolloidn. Zh. **35**, 1090 (1973).
19. S. O. Yesylevskyy, L. V. Schäfer, D. Sengupta, and S. J. Marrink, PLoS Comput. Biol. **6**, 1000810 (2010). https://doi.org/10.1371/journal.pcbi.1000810
20. G. Srinivas, S. O. Nielsen, P. B. Moore, and M. L. Klein, J. Am. Chem. Soc. **128**, 848 (2006).
21. M. Ndao, F. Goujon, A. Ghoufi, and P. Malfreyt, Theor. Chem. Acc. **136**, 1 (2017). https://doi.org/10.1007/s00214-016-2038-y
22. F. Grunewald, G. Rossi, A. H. de Vries, et al., J. Phys. Chem. B **122**, 7436 (2018).
23. G. Rossi, P. F. J. Fuchs, J. Barnoud, and L. Monticelli, J. Phys. Chem. B **116**, 14353 (2012).
24. A. M. Luz, T. J. P. dos Santos, G. D. Barbosa, et al., Colloids Surf., A **651**, 129627 (2022).
25. W. C. Swope, M. A. Johnston, A. I. Duff, et al., J. Phys. Chem. B **123**, 1696 (2019). https://doi.org/10.1021/acs.jpcb.8b11568
26. S. Yada, T. Suzuki, S. Hashimoto, and T. Yoshimura, Langmuir **33**, 3794 (2017).
27. E. A. Crespo, L. F. Vega, G. Perez-Sanchez, and J. A. P. Coutinho, Soft Matter **17**, 5183 (2021).
28. J. Chanda and S. Bandyopadhyay, J. Phys. Chem. B **110**, 23482 (2006).
29. M. J. Abraham, D. van der Spoel, E. Lindahl, and B. Hess, and the GROMACS development Team, GROMACS User Manual Version 2019.2. http://www.gromacs.org.
30. P. C. T. Souza, R. Alessandri, J. Barnoud, et al., Nat. Methods **18**, 382 (2021).
31. H. J. C. Berendsen, J. P. M. Postma, W. F. van Gunsteren, et al., J. Chem. Phys. **81**, 3684 (1984).
32. W. Humphrey, A. Dalke, and K. Schulten, J. Mol. Graph. **14**, 33 (1996).
33. P. O. Sorina and A. I. Victorov, J. Mol. Liq. **414**, 126229 (2024) https://doi.org/10.1016/j.molliq.2024.126229.
34. A. I. Victorov, in *Thermodynamics of Liquid–Vapor Equilibrium,* Ed. by A. G. Morachevskii (Khimiya, Leningrad, 1989) [in Russian].
35. A. I. Victorov, J. Chem. Eng. Data **59**, 2995 (2014).
36. A. I. Victorov and A. Fredenslund, Fluid Phase Equilib. **66**, 77 (1991).
37. N. Smirnova and A. Victorov, in *Equations of State for Fluids and Fluid Mixtures,* Ed. by J. V. Sengers, R. F. Kayser, C. J. Peters, and H. J. White (Elsevier Science, Amsterdam, 2000), p. 255.
38. C. Tsonopoulos, Fluid Phase Equilib. **156**, 21 (1999).
39. S. Zeppieri, J. Rodríguez, and A. L. López de Ramos, J. Chem. Eng. Data **46**, 1086 (2001).
40. P. A. Barneveld, J. M. H. M. Scheutjens, and J. Lyklema, Langmuir **8**, 3122 (1992). https://doi.org/10.1021/la00048a044
41. S. M. Oversteegen and F. A. M. Leermakers, Phys. Rev. E **62**, 8453 (2000).
42. S. Ono and S. Kondo, *Molecular Theory of Surface Tension in Liquids* (Springer, Berlin, 1960).

Translated by Sh. Galyaltdinov